ELSEVIER

Journal of Nuclear Materials 264 (1999) 20–28

journal of nuclear materials

Assessment of hydrogen embrittlement of Zircaloy-2 pressure tubes using unloading compliance and load normalization techniques for determining *J–R* curves

J.S. Dubey *, S.L. Wadekar, R.N. Singh, T.K. Sinha, J.K. Chakravartty

Materials Science Division, Bhabha Atomic Research Centre, Trombay, Mumbai 400 085, India

Received 13 March 1998; accepted 4 August 1998

Abstract

The fracture toughness of unirradiated cold pilgered pressure tubes (PT) has been studied as a function of temperature and hydrogen levels. Two methods of *J–R* curve evaluation, from small curved compact tension specimen, have been employed. In addition to the single sample unloading compliance method (298–473 K), a recently developed load normalization technique, using LMN function, has been used for temperature upto 548 K. The effect of circumferential hydrides on fracture toughness parameters has been studied. The results of both the techniques are compared to find out the suitability of load normalization method in such hydrogen embrittlement studies. The results show large deleterious effects of circumferential hydrides at lower temperatures and gradual restoration of toughness with increase in temperature. The study also shows that load normalization can be used to evaluate *J–R* curve in the cases where slow stable crack growth takes place. Hydrogen embrittlement can be evaluated using load normalization method for temperatures higher than 423 K.

1. Introduction

The pressurized heavy water reactor (PHWR) core has hundreds of pressure tubes (PT) made of cold worked Zircaloy-2 or Zr–2.5Nb alloy, which serve as the primary in-core containment for the reactor fuel and the heavy water coolant. Pressure tubes operate under demanding service conditions. They carry heavy water coolant at temperature in the range of 533–583 K, at a pressure of around 10 MPa and see fast neutron flux of about 3.2×10^{17} n/m^2 s [1]. A Zircaloy-2 PT has inner diameter of about 82.6 mm and a wall thickness of 4.0 mm and is around 6 m in length. The pressure tubes primarily see hoop stress (~105 MPa) and longitudinal stress (~55 MPa) but added to these are the bending loads due to fuel elements weight and any residual stresses present due to mechanical roll joints near the end fittings. Due to such operating environment, the pressure tubes undergo irradiation hardening and embrittlement, irradiation enhanced creep, irradiation growth, diametral creep, axial creep and sag [2]. The pressure tubes also pick up deuterium generated in the corrosion reaction with hot heavy water. Zircaloy-2 PT, in as fabricated conditions, have hydrogen level in the range of 10–15 ppm and during the service they may pick up hydrogen upto a level more than 100 ppm [3]. The low solubility of hydrogen in zirconium at lower temperatures, hydride formation in the zirconium metal, and the large diffusivity of hydrogen give rise to typical hydrogen embrittlement and delayed hydride cracking problems in the zirconium alloys [4]. Older Indian PHWRs, up to KAPP-1, use cold worked Zircaloy-2 as a material of pressure tube. For reactors KAPP-2 onwards, the material for pressure tubes is cold worked Zr–2.5 Nb.

One of the main design and operational requirement is to preclude any unstable fracture of pressure tubes during operation. Several studies have reported such analysis based on fracture mechanics principles and the slit burst tests in pressure tube segments [4–13]. It has

* Corresponding author. Tel.: +91-22 556 3060; fax: +91-22 556 0750, +91-22-556 0534; e-mail: mechmet@magnum.barct1.ernet.in.

0022-3115/99/$ – see front matter
PII: S0022-3115(98)00487-5

been found that the hydrogen embrittlement in zirconium alloys depends mainly upon the amount of hydrogen present in matrix, hydride morphology, orientation, and its distribution, and the texture, strength and fracture toughness of the zirconium matrix itself [4,5]. Apart from these, the external factors such as temperature, state of stress, presence of stress gradients and temperature gradients are also of prime importance in hydrogen embrittlement [4]. Therefore, the evaluation of fracture toughness degradation due to hydrogen ingress and irradiation damage over a range of temperatures continues to be of interest in structural integrity analysis.

Any kind of fracture mechanics approach would require the material resistance to crack growth initiation and its further propagation form a preexisting flaw. These data are normally generated by testing specimen of standard geometry to find out the crack tip characterizing parameters at these critical events. The cases, which show slow stable crack growth, J-integral parameter, and $\mathrm{d}J/\mathrm{d}a$, have been found to suitable characterizing parameters. The materials resistance to initiation of crack growth is expressed as J_{IC} and the crack growth resistance is evaluated in terms of $\mathrm{d}J/\mathrm{d}a$ values.

The tests employed to obtain J–R curve can be either multi-specimen testing or single sample J-integral tests. In single sample fracture toughness testing the on-line or continuous crack monitoring is required. This is done generally by unloading compliance measurements or by electric potential drop methods. Both of these techniques pose difficulties for use at higher temperatures and in aggressive environment. Recently, Grigoriev and co-authors [14] have proposed a notched tubular pin-loading tension (PLT) specimen suitable for fracture toughness evaluation of thin-walled tubular material. A 3D FEM analysis, giving details of more accurate estimation of J and COD, for PLT specimen, from load–load line displacement (LLD) record has been carried out by Ben Dhia et al. [15].

1.1. Load normalization technique for J–R curve determination

Load normalization method [16–19], which is based on the Key Curve approach [20], does not need on-line crack monitoring unit. It uses single specimen LLD record for the evaluation of J–R curve. The method is based upon the principle of load separation developed by Ernst et al. [21]. This technique has been demonstrated for several specimen geometry and for various materials having different work hardening behaviors by Sharobeam and Landes [22,23]. According to this principle, the load (P) may be written as a function of crack length (a) and plastic deformation (v_{pl}), by two separate multiplicative functions

$$P = G(a/W)H(v_{pl}/W), \tag{1}$$

where W is the specimen width. The plastic load line displacement can be expressed as

$$v_{pl} = v - v_{el} = v - PC(a/W), \tag{2}$$

where $C(a/W)$ is the elastic compliance, and is a function of actual crack length.

A normalized load (P_N) can then be defined as a function of only plastic displacement:

$$P_N = P/G(a/W) = H(v_{pl}/W). \tag{3}$$

The geometry calibration function $G(a/W)$ is dependent on the specimen geometry and can be determined from the J calibration [22,24]

$$G(a/W) = BW(b/W)^{\eta_{pl}}, \tag{4}$$

where uncracked ligament length $b = W - a$ and η_{pl} is the geometry correction factor, which depends only weakly on material properties. It has been shown that η_{pl} is independent of crack growth and has the value of 2.130 for compact tension specimens [22–24]. Several kinds of material deformation functions $H(v_{pl}/W)$ have been proposed, but Landes et al. have demonstrated that LMN function gives good fit over the large range of plastic displacement values [16]. The LMN function is given by

$$P_N = \frac{[L + M(v_{pl}/W)]}{N + (v_{pl}/W)}(v_{pl}/W). \tag{5}$$

The technique involves first finding the P_N verses v_{pl}/W, based on initial crack length from the P-LLD data. Thereafter for few initial points, points B, P_N values, are recalculated after allowing crack growth due to blunting. At the final point, point A, the final crack length is known, as it can be physically measured after the J test, so there actual P_N is known. As for LMN function to be defined at least, three points are required. The third set of intermediate points, point C, is chosen at an intermediate value of v_{pl}/W, e.g. $\frac{1}{3}$ of $(v_{pl}/W)_{max}$. The P_N at these intermediate points are not known to any close approximation as is the case with points taken for blunting. Therefore, a range of P_N is taken at these intermediate C points. The parameters L, M, and N are calculated for final point, set of blunting points, and one of these intermediate points. This is repeated for all the intermediate calibration points. The fitted LMN curve is compared for their deviation from these calibration points. The value of L, M, and N, giving the best fit, defines the function $H(v_{pl}/W)$. Once $H(v_{pl}/W)$ is known $G(a/W)$ can be calculated for each point of P–LLD curve which will give the value of crack extension at each point. Also from the P–LLD plot the $J_{elastic}$ and $J_{plastic}$ values can be found out as detailed in ASTM E813-87. The detailed flow sheet and methodology has been summarized by Landes et al. in Ref. [16].

Though there is a good amount of data available, on the fracture behaviour of hydrided and irradiated pressure tube materials in the literature, the data are mainly for the extruded and cold drawn PT and obtained by electric potential drop methods for monitoring the crack growth [5–13]. The Indian PHWRs use the pressure tubes, which are fabricated from a different processing route involving cold pilgering of extruded tubes. This report includes fracture toughness test results of Zircaloy-2 pressure tubes made by nuclear fuel complex (NFC). This work had threefold aim. Firstly, to assess the fracture toughness of Zircaloy-2 pressure tubes made by a different fabrication route as a function of hydrogen content and temperature. Secondly, to use and compare two different techniques for evaluation of *J–R* curves, namely unloading compliance (up to 473 K) and load normalization method (up to 548 K). Lastly, though this study employs unirradiated pressure tubes with predominantly circumferential hydrides, it was aimed at testing the usefulness of load normalization technique for *J–R* curve evaluation in hydrogen embrittlement studies. This study also gives a more accurate data for the effect of cicumferential hydrides and temperature on fracture behaviour of cold pilgered Zircaloy-2 pressure tubes.

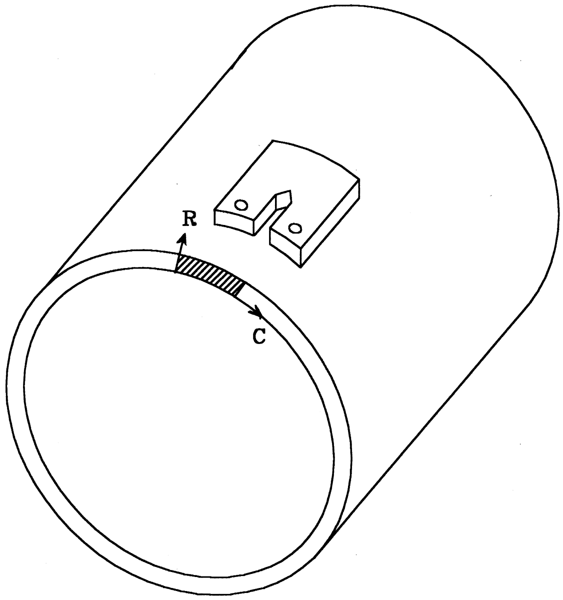

Fig. 1. Schematic diagram of pressure tube segment with curved compact tension specimen showing its orientation. It also depicts the radial (*R*) and circumferential (*C*) directions and the hatched area, which are shown in the metallographs.

2. Experimental

2.1. Material

The pressure tubes for Indian PHWRs are fabricated at the Nuclear Fuel Complex (NFC). The fabrication route for Zircaloy-2 includes double vacuum arc melting, extrusion, and two stage cold pilgerings with an intermediate annealing [1]. The mean composition was 1.5 Sn, 0.12 Fe, 0.1 Cr, 0.05 Ni and 0.12 O (all in wt%). This fabrication route gives predominantly radial basal pole texture [1]. The pressure tube sections were cut into rings. From these rings, 17 mm wide and 4 mm thick Curved Compact Tension (CT) specimens, with knife-edges on the front face for attaching the COD gage, were obtained. The curved compact tension specimens have also been used in earlier studies [6]. The samples were in C–L orientation i.e. the normal to crack plane was in circumferential direction and the direction of crack growth was longitudinal. The schematic drawing of the pressure tube segment, sample, and sample's orientation is shown in the Fig. 1. The CT specimens were polished and gaseous hydrogen charging was done to the level of about 60 and 110 ppm (wt%). The amount of hydrogen introduced in the samples was calculated from the volume of hydrogen gas absorbed during the charging process. The samples were given hydrogen homogenization treatment at 653 K for 48 h in a glass tube in-closure under helium atmosphere. The samples were polished to observe the hydride platelet distribution and density. Few CT specimens were left uncharged. In the as received condition, these samples are reported to have 10–15 ppm of hydrogen. The distributions of the hydride platelets, in the specimen, were as shown in Fig. 2. Uncharged sample (10 ppm H) showed no apparent hydrides, whereas at 60 and 110 ppm levels, nearly continuous circumferential hydrides can be seen. The density and continuity of hydrides are larger in the 110 ppm hydrogen charged samples. For the purpose of calculations material flow stress was taken to be 525 MPa at 298 K and 320 MPa at 548 K [1]. The material modulus has been taken to be 93 GPa at 298 K and 81 GPa at 548 K [6].

2.2. Single sample J_{IC} testing

The CT samples were fatigue precracked with a servohydraulic machine using a ΔK of 12–9 MPa $m^{1/2}$ and a load ratio of 0.1 up to an a/W ratio of around 0.6. The samples were tested as per ASTM E813-87 for evaluation of J–Δa curve by single sample unloading compliance technique. The K calibration of flat sample was used as the curvature due to the tube radius in the sample introduces less than 10% change in the stress intensity factor for small sized sample [6]. A small tubular furnace was fabricated to carry out the elevated temperature tests with COD gage. The tests with COD gage were restricted upto the temperature of 473 K due

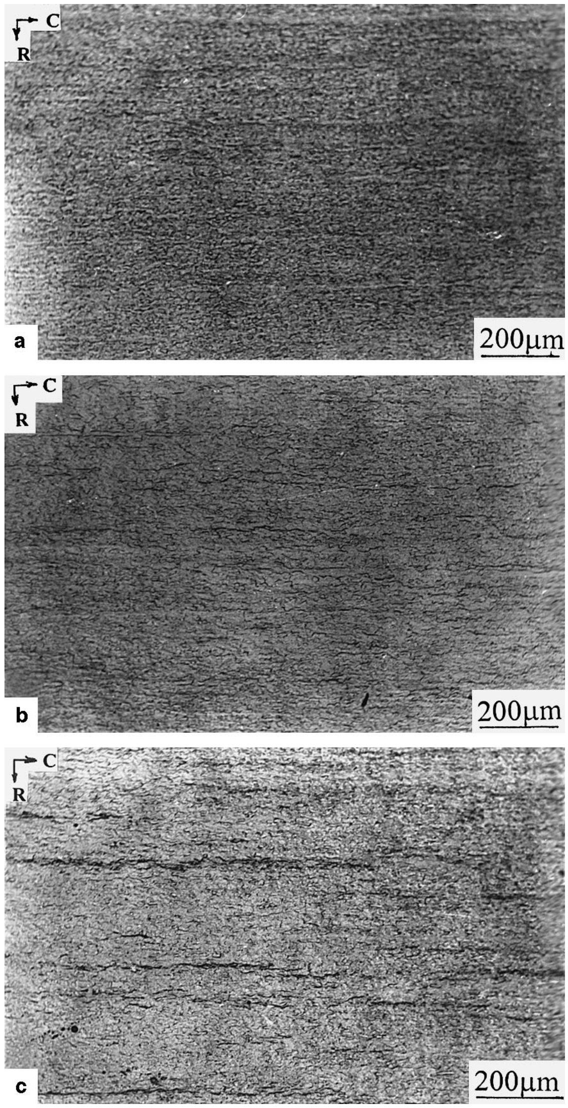

Fig. 2. Metallograph showing the hydride platelet distribution in unirradiated Zircaloy-2 pressure tube specimens, on the radial-circumferential plane, for (a) 10 ppm (b) 60 ppm (c) 110 ppm hydrogen levels.

to the limitation of COD gage. The single sample J_{IC} tests were carried out using computer controlled machine controller and data acquisition system. The load (P) and LLD were recorded along with on-line unloading compliance measurements as per ASTM E813-87. The J–Δa curve obtained gave the values of J_{IC} and dJ/da values. A sample plot for the single sample J-integral test is shown in the Fig. 3. After the J tests, the specimens were fatigue cracked to delineate the crack extensions. The initial and final crack lengths were physically measured using a travelling microscope.

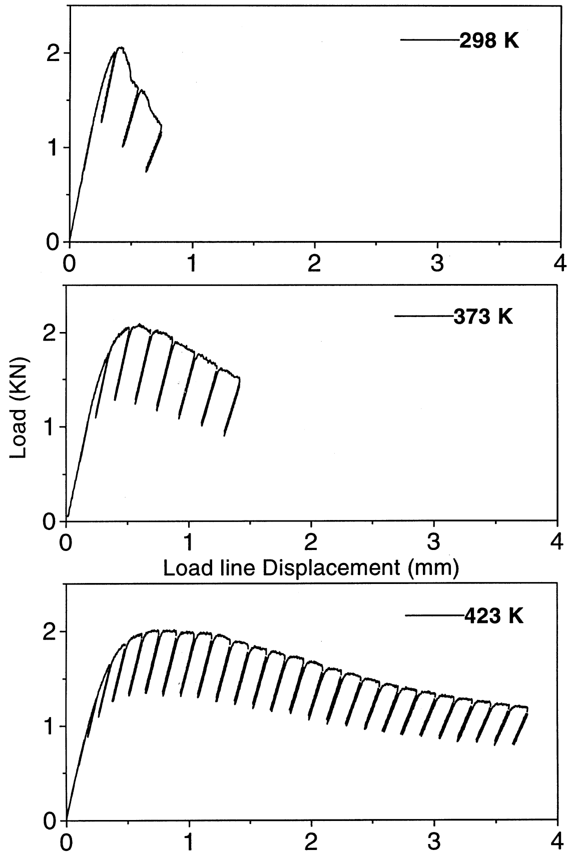

Fig. 3. Load–load line displacement plots for Zircaloy-2 specimen charged with 60 ppm of hydrogen during J–R curve determination using unloading compliance.

2.3. Load normalization method for J–R curve evaluation

For temperatures upto 473 K, the same data of P–LLD as obtained in single sample J test were used, but without using unloading compliance measurement portions. This data was re-analyzed using load normalization technique discussed above. At temperature of 548 K, the COD gage was not used and LLD was obtained form the actuator displacement after deducting the extraneous displacements. This extraneous displacement could be found out by pulling an identical uncracked sample under similar test conditions. A sample plot of P_N based on initial crack length verses v_{pl}/W is shown in Fig. 4. Also shown in Fig. 4 are the LMN fit calibration points, which includes a set of forced blunting points B, near crack blunting region, final point A, and a set of intermediate calibration points C. Fig. 4 also compares the fitted LMN function with the normalized load curve.

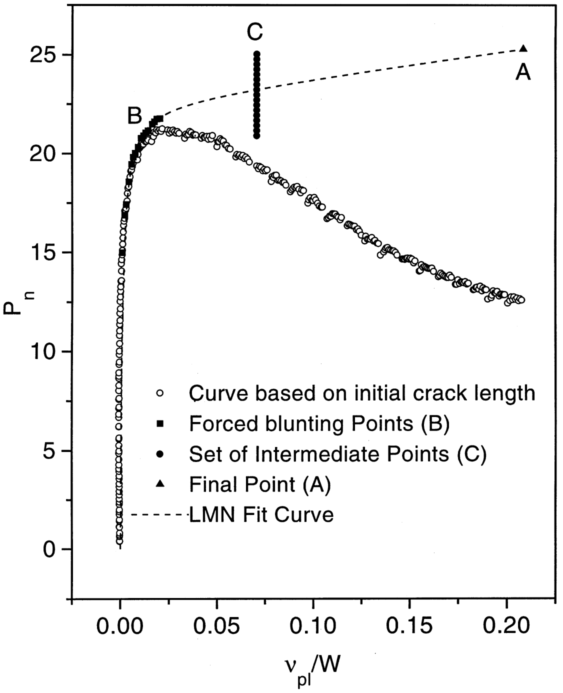

Fig. 4. Plot showing normalized curve, *LMN* function fit calibration points and final fitted curve for Zircaloy-2 specimen (60 ppm hydrogen) tested at 423 K.

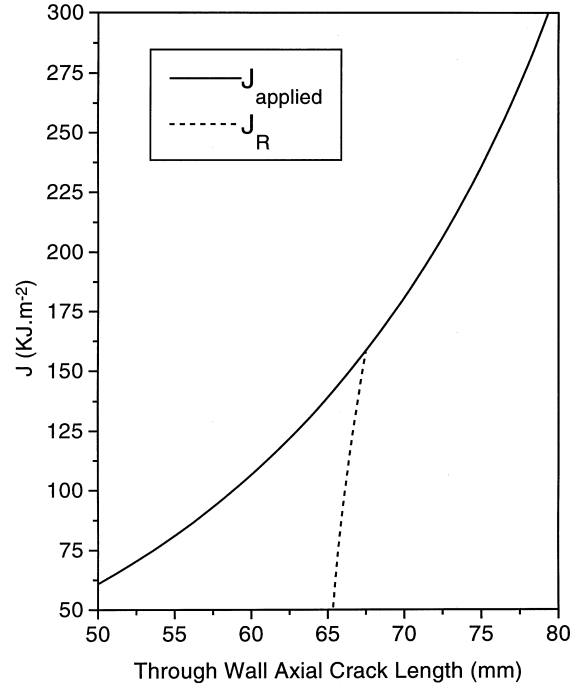

Fig. 5. Evaluation of critical crack length for unirradiated Zircaloy-2 pressure tube charged with 60 ppm hydrogen at hoop stress of 103 MPa at 473 K.

2.4. Critical crack length evaluation

The critical crack length (CCL) was estimated using the Dugdale plastic strip yield Model and using the stress intensity factor, modified by Folias factor for through wall axial cracks in pipes [25,6]. The value of J_{applied} as a function of axial crack length was plotted. On this plot, the *J–R* curves obtained by fracture toughness tests were superimposed, as shown in Fig. 5. The point of near tangency between these curves was taken as the critical crack length. CCL values, obtained here, do not take into account any degradation in toughness due to irradiation and environment. Therefore, these CCL values are only indicative of the extent of toughness degradation due to hydrogen ingress in the Zircaloy-2 pressure tube specimen.

3. Result and discussion

3.1. Specimen size considerations

In order to maintain the plane strain condition and J dominance, near the crack tip, at the point of crack growth initiation, it is usually taken that the minimum specimen size should be [26–28]

$$B, b > \rho \frac{J}{\sigma_{\mathrm{f}}}, \tag{6}$$

where

$\rho = 25$ for bend and compact tension geometry;
B = specimen thickness;
b = remaining ligament;
σ_{f} = material flow stress, usually taken to be the average of yield strength and tensile strength.

In addition, for the J-controlled crack growth [26–28] during the *J–R* curve evaluation it is taken that

$$\Delta a \leqslant \alpha(W - a_o), \tag{7}$$

$$\omega = \frac{b}{J}\frac{\mathrm{d}J}{\mathrm{d}a}, \quad \omega \gg 1, \tag{8}$$

where

W = specimen width
a_{o} = initial crack length.

The values of α are usually taken to be in the range 0.06–0.1 [26,27]. The value of ω is usually taken to be near 5–10 for compact and bend geometry [26].

In this study, the test specimen thickness was limited to that of actual pressure tube thickness which is around 4.0 mm. Due to the small sample thickness (4.0 mm), the maximum J value where plane strain condition and J dominance is maintained, near the crack tip, ranges from about 100 kJ m^{-2} at room temperature to less than

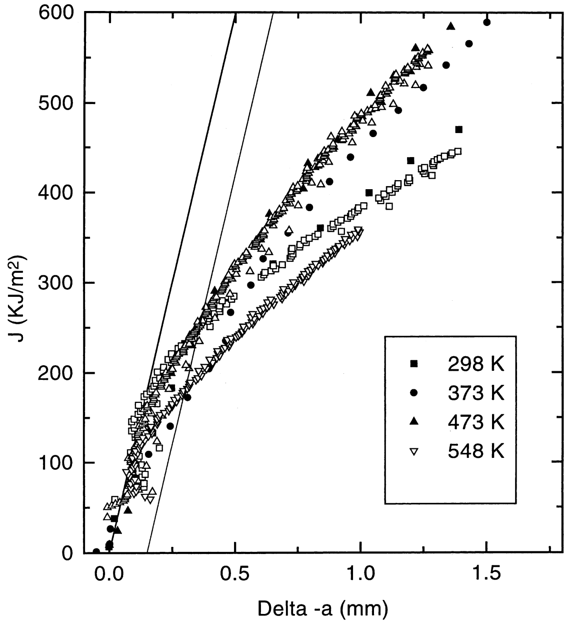

Fig. 6. J–R curves obtained by single sample unloading compliance (filled symbols) and load normalization method (open symbols) for as fabricated Zircaloy-2 pressure tubes.

55 kJ m^{-2} at 548 K. Therefore, the J_{IC} values which were in this range may be taken to give the approximate K_{IC} values, which is a material property. The remaining ligament sizes were about 5–6 mm and this limited the amount of crack growth which could be taken to J-controlled to less than 0.6 mm. The values of ω in these J–R curve tests, even at the higher temperature, were also less than 3.6. All these facts indicate that J–R curves obtained in this study are not the material property but they give the case specific values for the pressure tubes.

3.2. Fracture toughness results

The J–Δa curves obtained for uncharged samples are shown in the Fig. 6. The uncharged samples, which had 10–15 ppm hydrogen, showed high crack initiation toughness and dJ/da values at all the test temperatures. The values of J_C ranged from 270 to 300 kJ m^{-2} for temperature upto 473 K. The crack growth resistance, signified by dJ/da values, showed larger increase with increase in temperature. This may be explained by the fact that crack initiation in unirradiated and unhydrided Zircaloy-2 is by strain controlled ductile crack growth [29] and the near tip fracture strains are likely to change little in this temperature range. Increased dJ/da at higher temperatures appears to be due to increased plasticity ahead of crack tip at higher temperatures. The value of J_{IC} and dJ/da obtained is given in Table 1 for all the tests.

Severe embrittlement due to hydride formation is very much evident from the sharp reduction in J_C and dJ/da values. The J–Δa curve for the specimen charged with around 60 and 110 ppm of hydrogen is as shown in Figs. 7 and 8, respectively. The increase in temperature restores the toughness of material and at 473 K the effect of circumferential hydrides on fracture toughness is much smaller, though here also the J_C values continue to be less than that of uncharged sample. A monotonous increase in dJ/da values, shown in Fig. 9, shows that the crack growth toughness increases with the increase in temperature. Up to 373 K, the effect of hydrogen ingress seems to saturate at the 50 ppm or less hydrogen level. Any further increase in hydrogen does not seem to have any noticeable effect on the toughness levels. It can be observed that at temperatures below 423 K the embrittlement due to hydrogen presence is markedly large. The value of $K_{JC} = (J_{IC}\,E)^{0.5}$, is shown in Fig. 10 for all the specimen.

At room temperature and 373 K, the toughness parameters for 100 ppm H specimen remain unchanged from that of at 50 ppm hydrogen level. However, at higher temperature the degradation in crack initiation toughness and dJ/da values was observed. This may be due to excess hydride volume fraction present in material charged with 100 ppm of hydrogen. The specimens with 110 ppm H, show much less toughness even at 423 K in comparison to uncharged material response.

The hydrogen charged specimen, in this study, had predominantly circumferential hydrides. In the tests

Table 1
Fracture toughness parameters as a function of hydrogen content and temperature (CCL values are for hoop stress value of 103 MPa)

T (K)	Uncharged specimen 10–15 ppm H			60 ppm H			110 ppm H		
	J_C (kJ m^{-2})	dJ/da (MPa)	CCL (mm)	J_C (kJ m^{-2})	dJ/da (MPa)	CCL (mm)	J_C (kJ m^{-2})	dJ/da (MPa)	CCL (mm)
298	275	207	86	35 ($K_{JC}=57$ MPa $m^{1/2}$)	24	50	40 ($K_{JC}=60$ MPa $m^{1/2}$)	44	58
373	270	295	>87	67 ($K_{JC}=78$ MPa $m^{1/2}$)	97	65	67 ($K_{JC}=78$ MPa $m^{1/2}$)	72	69
473	–	–	–	152	157	81	100	91	77
573	306	350	>87	182	280	–	–	–	–
548	186	285	–	–	–	–	213	258	–

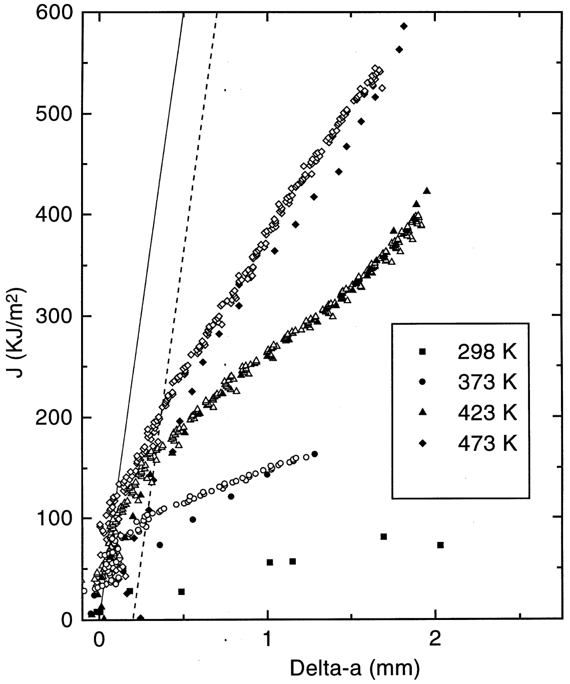

Fig. 7. *J–R* curves obtained by single sample unloading compliance (filled symbols) and load normalization method (open symbols) for Zircaloy-2 pressure tubes charged with 60 ppm of hydrogen.

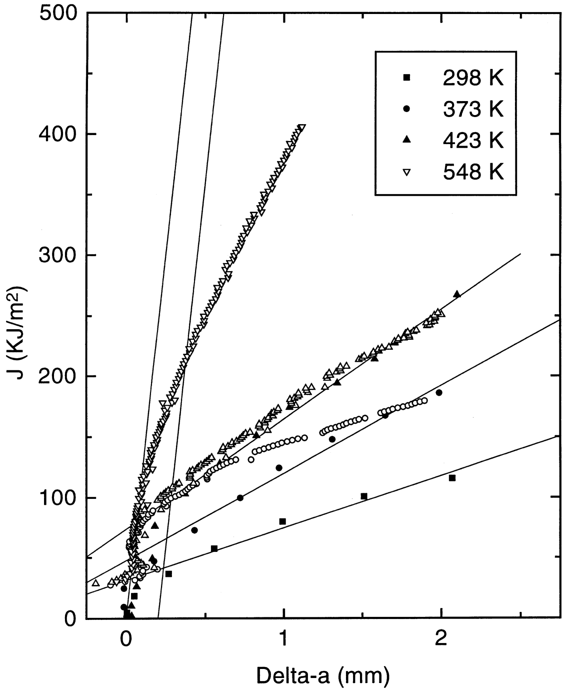

Fig. 8. *J–R* curves obtained by single sample unloading compliance (filled symbols) and load normalization method (open symbols) for Zircaloy-2 pressure tubes charged with 110 ppm of hydrogen.

carried out, a systematic change in both J_{IC} and dJ/da is seen. This is in contrast with difficulty reported in obtaining reproducible J_{IC} values for Zr–2.5Nb specimen testing [5]. In this study, value of K_{JC} at 373 K was about 78 MPa $m^{1/2}$. In comparison a study of Zircaloy-2 (60 μg/g H) with radial hydrides showed a maximum load fracture toughness of about 25–35 MPa $m^{1/2}$ [6,13]. This shows the more deleterious effect of radial hydrides in comparison to circumferential hydrides. As against relatively sharper change in fracture toughness in case of radial hydrides [13], the change in toughness is more gradual in case of circumferential hydrides. The value of K_{JC} obtained in this study for uncharged sample (125–155 MPa $m^{1/2}$) is higher than that reported by Huang [12] that is 90–110 MPa $m^{1/2}$. The tearing modulus for uncharged sample increased from about 53 at 298 K to 182 at 473 K. Huang [12] reported similar value at room temperature but lower values (90–120) at 473 K.

CCL calculated is also tabulated in Table 1. Fig. 11 shows the change in CCL values as a function of temperature and hydrogen content. Preliminary analysis [25] shows that fracture may take place by plastic collapse for crack lengths greater than 85–90 mm for uncharged specimen. The lowest CCL obtained is around 50 mm for hydrogen charged specimen at room temperature.

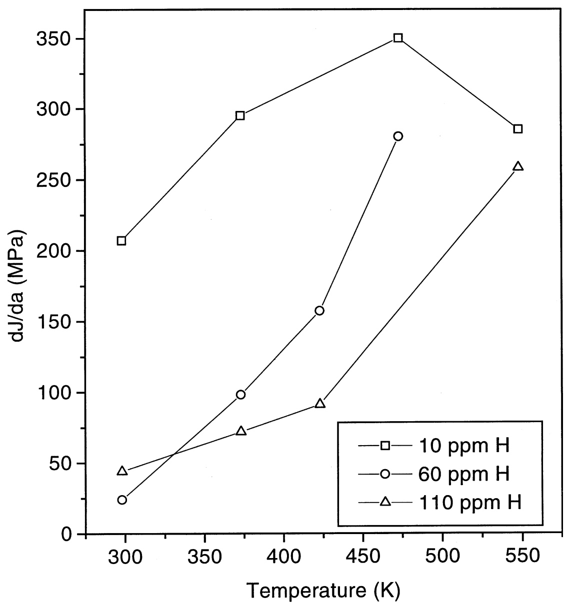

Fig. 9. Change in dJ/da values with temperature for unirradiated Zircaloy-2 pressure tubes, in C–L orientation, with circumferential hydrides.

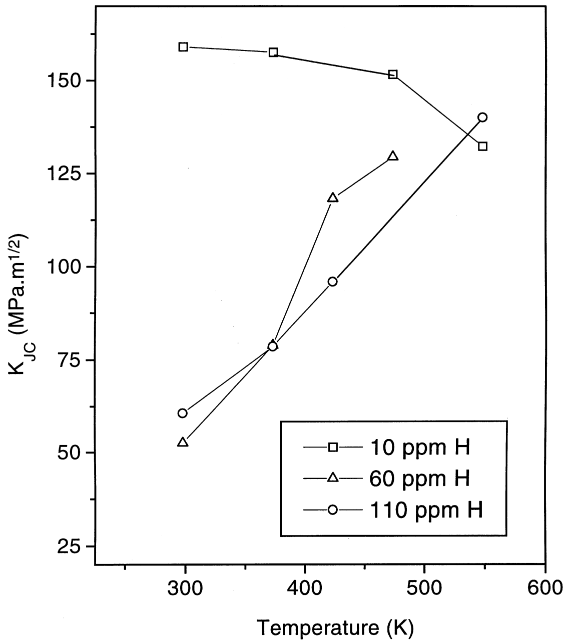

Fig. 10. Change in K_{JC} values with change in temperature for unirradiated Zircaloy-2 pressure tube specimens having circumferential hydrides.

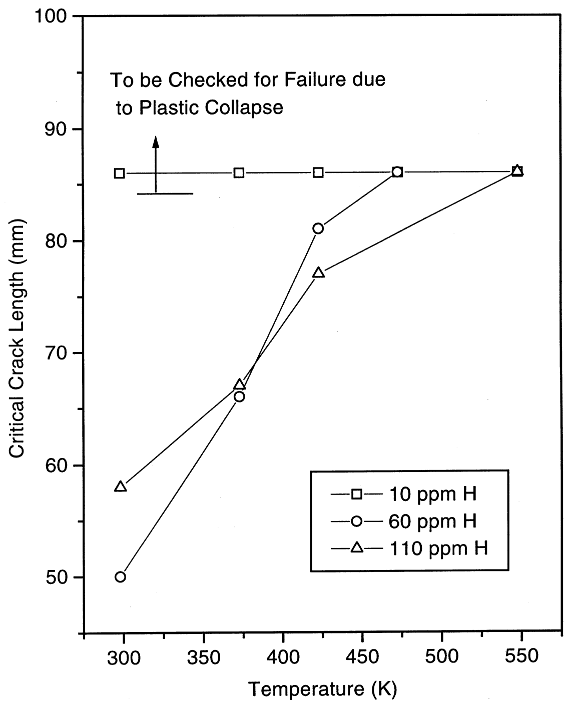

Fig. 11. Estimated critical through wall axial crack length for unirradiated pressure tubes, with circumferential hydrides, as a function of hydrogen content and temperature, from small specimen *J–R* curves.

The CCL values increase rapidly with temperature becoming more than 75 mm at 423 K.

3.3. Suitability of load normalization method

In the load normalization method, determination of *L*, *M*, and *N* constants is the key factor. The final point *A* is known from the Eq. (3). The forced blunting points *B* follow the blunting equation

$$J = m\sigma_f \Delta a, \tag{9}$$

where σ_f is the effective flow stress and m is the crack tip constraint factor, taken to be 2.0 in ASTM E813 (87). The value of m may differ from this in the case of some ductile materials, and may be empirically determined as detailed in EGF procedure [28] or as suggested by Landes [30]. The intermediate calibration points *C* have no fixed starting values. The best starting value reported for the *C* point is one third of the v_{pl}/W range and P_N value corresponding to the maximum at *B* points [16]. With this starting *C* point, the value P_N at point *C* is increased in steps to approach the best value. In this study it was found that the P_N value at the first *C* point if taken to be lower than maximum at *B* points and then increased in small intervals gave much better results. The average value of *L*, *M*, and *N* were found for each *C* point and corresponding function was plotted on actual calibration points. The point *C* which gave the best fit over all the calibration points (set of *B* points and point *A* taken together), was chosen and the average value obtained for *L*, *M*, and *N* at that step was taken to be the best-fit values. It was observed that it is better to range down the value of P_N at point *C* slowly to approach the best value. All these calculations and fittings were performed by writing a program on a personal computer with a graphics package available for repeated plotting of functions and curves.

For hydrogen charged specimens, the *J–R* curves obtained by the load normalization method and compliance method show quite good correlation at the temperatures greater than 423 K, as shown in Figs. 6–8. However, at the lower temperatures they do not fit well over the data. This can be expected as the *LMN* function represents slow stable crack growth. In the hydrogen charged samples, at lower temperatures, there is a rapid crack growth with small changes in normalized plastic displacement, which are difficult to be represented by such functional behaviour. The load normalization method thus gives an alternative way of obtaining *J–R* curves in the hydrogen charged samples at temperatures greater than 423 K. The ductile to brittle transition temperature in irradiated pressure tubes are reported to be in the range of 443–493 K [5,6,13]. It seems likely that the load normalization method could be extended to the testing of irradiated pressure tubes in this temperature range. As such, this method is a much simpler alternative, avoiding difficulties associated with the use of electric potential drop or COD gages in the hot cell or at elevated temperatures. For the uncharged specimens, load normalization technique gave good agreement in results at all the temperatures.

4. Conclusion

This study shows the deleterious effect of circumferential hydrides on the fracture toughness of unirradiated Zircaloy-2 pressure tubes. The circumferential hydrides have been found to be less damaging than radial hydrides. The crack growth initiation toughness of uncharged samples changes little over range of test temperature but dJ/da shows rapid increase. For temperature, less than 373 K, both 60 and 110 ppm hydrogen levels gave similar toughness values. At temperature greater than 373 K the 110 ppm specimen showed reduced toughness than the 50 ppm hydrogen level. The load normalization, by *LMN* function, gave good fit for temperature of 423 K and above in case of hydrogen charged specimen. For uncharged specimen, load normalization could be used at all the test temperature. The study also shows that load normalization can be used to evaluate J–R curve in the cases where slow stable crack growth take place. Hydrogen embrittlement can be evaluated using load normalization technique for temperatures higher than 423 K.

Acknowledgements

We wish to thank Dr S. Banerjee, Associate Director, Materials Group, Bhabha Atomic Research Centre, for his support and guidance during this work. We also thank Dr S.K. Roy, of our division for his help in experimental setup preparations.

References

[1] M.K. Asundi, S. Banerjee, Proceedings of the Symposium on Nuclear Fuel Fabrication, BARC, Bombay, India, 1988.
[2] E.F. Ibrahim, B.A. Cheadle, Can. Met. Quart. 24 (3) (1985) 273.
[3] D.D. Lanning, A.B. Johnson Jr., D.J. Trimble, S.M. Boyd, in: L.F.P. VanSwam, C.M. Eucken (Eds.), Zirconium in the Nuclear Industry: English International Symposium, ASTM STP 1023, ASTM, Philadelphia, 1989, p. 3.
[4] D.O. Northwood, U. Kosasih, Int. Metals Rev. 28 (2) (1983) 92.
[5] L.A. Simpson, C.K. Chow, in: R.B. Adamson, L.F.P. VanSwam (Eds.), Zirconium in the Nuclear Industry, Seventh International Symposium, ASTM STP 939, ASTM, Philadelphia, 1987, p. 579.
[6] C.K. Chow, L.A. Simpson, in: D.T. Read, R.P. Reed (Eds.), Fracture Mechanics: 18th Symposium, ASTM STP 945, ASTM, Philadelphia, 1988, p. 419.
[7] T. Asada, H. Kimoto, N. Chiba, Y. Kasai, in: C.M. Eucken, A.M. Garde (Eds.), Zirconium in the Nuclear Industry: Ninth International Symposium, ASTM STP 1132, ASTM, Philadelphia, 1991, p. 99.
[8] C.K. Chow, K.H. Nho, J. Nucl. Mater. 246 (1997) 84.
[9] C.K. Chow, L.A. Simpson, in: C.M. Hudson, T.P. Rich (Eds.), Case Histories Involving Fatigue and Fracture Mechanics, ASTM STP 918, ASTM, Philadelphia, 1986, p. 78.
[10] W.J. Langford, L.E.J. Mooder, Int. J. Pres. Ves. Piping 6 (1978) 275.
[11] F.H. Huang, J. Nucl. Mate. 207 (1993) 103.
[12] F.H. Huang, in: W.R. Corwin, F.M. Haggag, W.L. Server (Eds.), Small Specimen test Techniques Applied to Nuclear Reactor Vessel Thermal annealing and Plant Life Extension, ASTM STP 1204, ASTM, Philadelphia, 1993, p. 182.
[13] P.H. Davies, C.P. Stearns in: Fracture Mechanics: 18th Symposium, ASTM STP 905, ASTM Philadelphia, 1986, p. 379.
[14] V. Grigoriev, B. Josefsson, A. Lind, B. Roshborg , Scripta Metall. Mater. 33 (1) (1995) 109.
[15] A. Ben Dhia, J.B. Bai, D. Francois, Int. J. Pres. Ves. Piping 71 (1997) 189.
[16] J.D. Landes, Z. Zhou, K. Lee, R. Herrera, J. Testing Eval. 19 (1991) 305.
[17] J.D. Landes, R. Herrera, Int. J. Fracture 36 (1988) R9.
[18] R. Herrera, J.D. Landes, J. Testing Eval. 16 (5) (1988) 427.
[19] J.D. Landes, R. Herrera, Int. J. Fract. 36 (1988) R15.
[20] J.A. Joyce, H.A. Ernst, P.C. Paris, in: Fracture Mechanics: 12th Conference, ASTM STP 700, ASTM, Philladelphia, 1980, p. 222.
[21] H.A. Ernst, P.C. Paris, J.D. Landes in: R. Roberts (Ed.), Fracture Mechanics, 13th Conference, ASTM STP 743, Philadelphia 1981, p. 476.
[22] M.H. Sharobeam, J.D. Landes, Int. J. Fract. 47 (1991) 81.
[23] M.H. Sharobeam, J.D. Landes, Int. J. Fract. 59 (1993) 231.
[24] E.D. Reese, K.H. Schwalbe, Fat. Fract. Eng. Mater. Struct. 16 (3) (1993) 271.
[25] M.F. Kanninen, C.H. Popelar, Advanced Fracture Mechanics, Oxford University, Oxford, 1985, p. 289.
[26] J.W. Hutchinson, J. Appl. Mech. 50 (1983) 1042.
[27] R.L. Jones, J.R. Gordon, N.V. Challenger, Fat. Fract. Eng. Mater. Struct. 14 (1991) 777.
[28] K.H. Schwalle, B.K. Neule, T. Ingham, Fatigue Fract. Eng. Mater. Struct. 11 (1988) 409.
[29] C.E. Coleman, B.A. Cheadle, A.R. Causey, P.C.K. Chow, P.H. Davies, M.D. McManus, D.K. Rodgers, S. Sagat, G.V. Drunen, in: L.F.P. VanSwam, C.M. Eucken (Eds.) Zirconium in the Nuclear Industry: International Symposium, ASTM STP 1023, ASTM Philadelphia, 1989, p. 35.
[30] J.D. Landes, Fatigue Fract. Eng. Mater. Struct. 18 (11) (1995) 1289.